DR NISHA K. SHAH (Orcid ID : 0000-0003-0556-123X)

Article type : Research Article

Pyrimidine based pyrazoles as Cyclin-dependent kinase 2 inhibitors: Design, Synthesis and Biological Evaluation

Mayur K. Vekariya[a], Rajesh H. Vekariya[a], Pathik S. Brahmkshatriya[b], Nisha K. Shah[a]*

[a]*Department of Chemistry, Gujarat University, Ahmedabad, Gujarat 380009, India*

[b]*Institute of Organic Chemistry and Biochemistry, Academy of Sciences of the Czech Republic, v.v.i., Flemingovo nám. 2, 16610 Prague 6, Czech Republic*

* Corresponding author

Nisha K. Shah

Department of Chemistry,

Gujarat University, Ahmedabad, Gujarat 380009, India

Tel : (M) +91 9825312095, (O) +91 79 26300969

E-mail : nishchem2004@yahoo.in

Abstract

A series of new pyrimidine-pyrazole hybrid molecules were designed as inhibitors of cyclin-dependent kinase 2. Designed compounds were docked using Glide and the compounds showing good score values and encouraging interactions with the residues were selected for synthesis. They

This article has been accepted for publication and undergone full peer review but has not been through the copyediting, typesetting, pagination and proofreading process, which may lead to differences between this version and the Version of Record. Please cite this article as doi: 10.1111/cbdd.13334

were then evaluated using CDK2-CyclinA2 enzyme inhibition by a luminescent ADP detection assay. We show that of the 26 compounds synthesized and evaluated, at least 5 compounds were found to be highly potent (IC_{50}< 20 nM); which can be further optimized to have selectivity over other kinase isoforms.

Keywords: structure-based design, docking, cyclin-dependent kinase 2, pyrazole

1. Introduction

Controlling cell cycle by inhibiting various enzymes that normalize its progression is a smart strategy for treating cancer and other diseases accompanying with abnormal cellular production[1]. Cyclin-dependent kinases (CDKs) are one class of such serine/threonine protein kinases and are well known for their vital roles in the regulation of cell divisions. Action of these CDKs is tightly regulated at several levels: dealings with negative and positive regulatory partners, activation by phosphorylation or dephosphorylation, and shifts in their subcellular localization, etc. Cell cycle deregulation is often related with the CDK activity in many cancers[2]. For these reasons, CDKs have been targeted by numerous experimental anticancer therapeutics[3]. For example, palbociclib, a dual inhibitor of CDK4/CDK6, has recently been approved for the treatment of ER-positive and HER2-negative breast cancer[3]. Of the CDKs, CDK2 has been one of the most extensively studied members.

Several small molecules inhibitors of CDK2 have entered clinical trials. (Fig. 1)[4]. Many of them contain pyrimidine and pyrazole moieties in their backbone which interact with the key hinge residues. Moreover, pyrimidine and pyrazole analogues constitute an important class of bioactive molecules and as drugs also. In medicinal chemistry, both pyrimidine derivatives and pyrazole derivatives have been very well known for their biological potency. They demonstrate various types of pharmacological activities such as anti-cancer[5,6], anti-viral[7,8], anti-HIV[9,10], anti-hypertensive[11,12], anti-tubercular[13,14], diuretic [15,16], anti-bacterial[17,18], anti-fungal[19,20] and anti-epileptic[21,22] properties, and many classes of chemotherapeutic agents containing pyrimidine and pyrazolenucleus are in clinical trials.

Most of these inhibitors are designed either by structure-based drug design approach employing virtual screening/docking a large library of compounds or screening a small sub-set of focused library of compounds. In the present work, we combine both these strategies, i.e. knowledge-based approach (identifying the known pharmacophores for CDK2 inhibition) and structure-based drug design. To execute this, we identified novel CDK2 inhibitors with pyrazole and pyrimidine moieties embedded in a single molecule. Molecular docking of thus obtained focused virtual library of compounds led to identification of a series of new pyrimidine-pyrazole hybrid molecules, which were synthesized and evaluated in vitro for their CDK2-Cyclin A2 inhibitory activity using kinase system along with ADP-Glo Assay. We strongly feel that this approach is a better way to identify potential lead compounds which are good candidates for further evaluation for kinase selectivity profiling.

2. Experimental protocols

2.1. Design

2.1.1. Structure preparation

Protein structure coordinates were obtained from the RCSB Protein Data Bank (PDB Code 2R3J)[3]. Protein structures were prepared using the Protein Preparation Wizard in Maestro (Maestro v.10.1). Default settings were used, except that missing side chains were added, all crystallographic water molecules were removed and at the protein structure refinement step, exhaustive sampling was used in order to obtain a better H-bond assignment. Ligands were prepared using LigPrep tool with an Optimized Potentials for Liquid Simulations (OPLS_2005) force field. Their ionization states were generated at pH 7.0 ± 2.0 using Ionizer in LigPrep. Specific chiralities were retained during ligand preparations and stereoisomers per ligand were retained at a minimum value of 1.

2.1.2. Grid generation

Docking receptor grid was generated using Glide's Receptor Grid Generation module. Grids were generated keeping the default parameters of van der Waals scaling factor as 1.00 and charge cutoff as 0.25; which was subjected to OPLS 2005 force field. A cubic box of 10 × 10 × 10 dimension centered around the inhibitor in the active site was generated for each protein.

2.1.3. Docking

Standard precision (SP) ligand docking was carried out in Glide of Schrödinger-Maestro v10.1 within which penalties were applied to non-cis/trans amide bonds. Van der Waals scaling factor and partial charge cutoff was selected to be 0.80 and 0.15, respectively for ligand atoms. Final scoring was performed on energy-minimized poses and displayed as Glide score. Number of poses were limited to 5 per ligand.

2.2. Synthesis

All the analytical grade reagents and raw materials used were obtained from known marketable sources and were used without further purification. TLC was performed on silica gel 60 F254 plate (Merck, Germany) and visualization was done using iodine or UV light Column chromatography was performed using silica gel (60-120 mesh) from HPLC Chemicals (Mumbai, India). Melting points were determined in automatic melting point apparatus named Optimelt MPA100 and were uncorrected. Mass spectra were recorded in Waters Acquity TQD model, Waters USA where acetone was used as mobile phase with electron spray ionization (ESI) as ion source. ^{1}H-NMR and ^{13}C-NMR spectra were recorded on Bruker AV 400 MHz and 125 MHz spectrometer, respectively using DMSO-d6 as solvent and TMS as the internal reference. Spectral graphs obtained were shown in supporting data.

*2.2.1. Ethyl 2-((dimethylamino)methylene)-3-oxobutanoate (Intermediate-**A**)*

Ethylacetoacetate (26 g, 200 mmol) and DMF-DMA (26.2 g, 220 mmol) were heated at 80°C for 1 h in 100 ml three-necked flask. The reaction mixture was then quenched with *n*-pentane to remove unreacted material. Formation of product was confirmed by boiling point analysis. Reaction mixture was directly used for the next step without further purification to afford ethyl 2-((dimethylamino)methylene)-3-oxobutanoate (Intermediate-**A**) as dark brown liquid. Yield 90%; b.p. 180°C.

*2.2.2. 4-chloro-6-hydrazinylpyrimidine (**1**)*

4,6-Dichloropyrimidine (15 g, 100 mmol) in ethanol was charged in 250 ml three-necked flask and was cooled to 5°C. Hydrazine hydrate (4.7 ml, 120 mmol) was charged to the above flask dropwise. After complete addition of hydrazine hydrate, reaction mixture was stirred at room temperature for 90 minutes. The reaction mixture was filtered and washed with water to afford crude product which was recrystallized in ethanol to obtain 4-chloro-6-hydrazinylpyrimidine (**1**) as pale yellow solid. Yield 95%; Rf = 0.5 (hexane:ethyl acetate, 4:1); m.p. 164°C; ^{1}H NMR 8.83 (s, 1H), 8.17 (s, 1H), 6.76 (s, 1H), 4.50 (s, 2H); EI-MS (m/z): 145.02 (M+1).

*2.2.3. Ethyl 1-(6-chloropyrimidin-4-yl)-5-methyl-1H-pyrazole-4-carboxylate (**2**)*

To a solution of **1** (10.0 g, 69.2 mmol) in ethanol (100 mL) was added Intermediate-**A** (13.0 mL, 69.2 mmol) and the reaction mixture was stirred for 45 minutes. After that the reaction mixture was refluxed for 1 h. The reaction mixture was cooled and poured on crushed ice to obtain white solid as crude product which was filtered, dried and recrystallized from ethanol to obtain ethyl 1-(6-chloropyrimidin-4-yl)-5-methyl-1*H*-pyrazole-4-carboxylate (**2**) as white crystals. Yield 75%; Rf = 0.8 (hexane:ethyl acetate, 4:1); m.p. 180°C; ^{1}H NMR 9.936 (s, 1H), 8.492 (s, 1H), 8.238 (s, 1H), 4.216 (q, 2H), 2.782 (s, 3H), 1.312 (t, *J*=7.2 Hz, 3H). EI-MS (m/z): 268.07 (M+2).

*2.2.4. Ethyl 1-(6-(benzylamino)pyrimidin-4-yl)-5-methyl-1H-pyrazole-4-carboxylate (**3**)*

To a solution of **2** (20.0g, 74.9 mmol) in ethanol (100 mL) was added triethylamine (31.6 mL, 224 mmol) and benzylamine (8.2 mL, 75 mmol) and the mixture was stirred at 80^{o}C for 3 h. After complete consumption of both the reactants, reaction mixture was poured on ice-cold water. Resultant white precipitates were filtered off, dried and recrystallized with ethanol to afford Ethyl 1-(6-(benzylamino)pyrimidin-4-yl)-5-methyl-1*H*-pyrazole-4-carboxylate (**3**) as white solid. Yield 95%; Rf = 0.35 (hexane:ethyl acetate, 5:5); m.p. 188-192°C; ^{1}H NMR 9.912 (s, 1H), 8.432 (s, 1H), 8.212 (s, 1H), 7.32-7.22 (m, 5H), 4.204 (s, 2H), 4.106 (q, *J*=7.2 Hz, 2H), 2.122 (s, 3H), 1.312 (t, *J*=7.2 Hz, 3H); EI-MS (m/z): 338.47 (M+1).

*2.2.5. 1-(6-(benzylamino)pyrimidin-4-yl)-5-methyl-1H-pyrazole-4-carboxylic acid (**4**)*

To a previously cooled solution of **3** (22.0g, 65.2 mmol) in methanol:water (2:1) at 0-5^{0}C, lithium hydroxide (7.8g, 326 mmol) was added portion wise. After completion of addition, the reaction mixture was stirred at room temperature for 24 h. After completion of reaction, reaction mixture was poured on ice-cold water and acidified with 1N HCl. Precipitates formed were filtered, washed

with water and dried to afford 1-(6-(benzylamino)pyrimidin-4-yl)-5-methyl-1*H*-pyrazole-4-carboxylic acid (**4**) as white solid. Yield 96%; Rf = 0.30 (hexane:ethyl acetate, 3:7); m.p. 182°C; ^{1}H NMR 10.824 (s,1H), 9.932 (s, 1H), 8.422 (s, 1H), 8.12 (s, 1H), 7.32-7.22 (m, 5H), 4.211 (s, 2H), 2.102 (s, 3H); EI-MS (m/z): 310.04 (M+1).

2.2.6. 1-(6-(benzylamino)pyrimidin-4-yl)-5-methyl-1H-pyrazole-4-carboxamide

*derivatives (**5a-5z**)*

To a stirred solution of **4** (1mmol) in DMF was added HOBT (0.7 mmol) under anhydrous conditions at room temperature. EDC.HCl (1.5 mmol) was added to the above reaction mixture and stirred for 15 minutes. Triethylamine (3.0 mmol) was added and to the reaction mixture and it was further stirred for 5 minutes. After this, the corresponding amine (1.0 mmol) was added and reaction mixture was allowed to stir at room temperature for 1 to 2 h. Reaction was monitored on TLC. After completion of reaction, the reaction mixture was poured in cold-water and extracted with ethyl acetate twice. Combined organic layer was dried over sodium sulphate and concentrated to get crude product which was purified by column chromatography using ethyl acetate: hexane mobile phase and recrystallized from ethanol to obtain title compounds (**5a-5z**).Physical data of all targeted compounds were available in supporting data.

2.2. Biology

The CDK2-CyclinA2 enzyme inhibition assay was measured by a luminescent ADP detection assay using CDK2/CyclinA2 Kinase Enzyme System with ADP-Glo™ Kinase Assay kit (Promega Corporation, USA)[23]. The assay was performed in a volume of 50 µL at room temperature in 384-well flat bottom white polystyrene plates. The final concentrations of the assay ingredients were 25 ng CDK2-Cylin A2, 100 µg histone substrate, and 50µMATP. The compounds were dissolved in DMSO and added to the reaction mixture at eight different concentrations with the highest concentration of 20 µM for Roscovitine and 100 µM for the rest of the targeted compounds. DMSO concentration was maintained 1% in all the test concentrations irrespective of the dilutions. Continuous kinetic monitoring of enzyme activity was performed on VICTOR Multilabel Luminescence Reader (Perkin elmer, USA). The experiment was carried out in duplicate and the percent inhibition of enzyme activity was calculated for all the compounds at each concentration. The IC_{50} values were obtained from the non-linear curve fitting of the plot of percent inhibition versus inhibitor concentration [I] using the equation, % inhibition = 100/{1+ (IC_{50}/[I])k}, where k is the Hill slope in Graphpad Prism software. Bio assay results of Roscovitine was briefly shown in supporting data.

3. **Results and Discussion**

3.1 Computational results

ADME properties were predicted using *Qikprop* (Shrodinger) for all targeted compounds and the results obtained as shown in Table 1. All compounds showed drug like properties with no violation of Lipinski's rule of five. The Lipinski's rule of five values for all compounds were also tabulated in Table 1. All compound possess satisfactory pharmacokinetic properties (ADME). All compound have shown good percentage (83.302–100%) of human oral absorption. The projected aqueous solubility (QP log S) parameter directs all compounds possess permissible scores except some compound **5k**, **5p**, **5r**, **5x**. Similarly all compound exhibit good blood–brain barrier permeability

(QP log BB) values. The predicted IC_{50} value of HERG K+ channel blockage (QP logHERG) depicted admirable range of values.

Cyclin-dependent kinase 2 protein (PDB Code 2R3J) was used for docking the designed compounds into the active site of the protein. An in-house database of 100 compounds, which were designed based on the common pharmacophoric requirements for CDK2 inhibition, was used for docking. All compounds were docked using Glide-SP protocol and rescored using Glide-XP. Encouragingly, some of the compounds showed very good scores and showed favourable interactions with the neighbouring residues. It was also encouraging to see a satisfactory correlation between Glide score and pIC_{50} (r = 0.73, Table 2). Compounds which showed favourable interactions and good Glide score along with pharmacokinetic properties were then selected for synthesis. All compounds were found to have good glide score vary from -6.235 to -9.014. Fig. 2 shows docked poses of few representative molecules which were part of the synthesized target compounds. It was encouraging to see that most of the docked poses consistently showed interactions with the hinge residue (Leu83) with two strong hydrogen bonds. Along with this the compounds also interacted with Leu134, Ile10 and Phe82 with dispersion interactions.

3.2. Chemistry

The synthetic methodology for the pyrimidine pyrazole hybrid molecules is shown in **Scheme 1**. Synthesis of Enaminone intermediate through*N*,*N*-Dimethylformamide dimethyl acetal (DMF-DMA) approach [24] was a primary step towards the formation of key scaffold i.e. ethyl 1-(6-chloropyrimidin-4-yl)-5-methyl-1*H*-pyrazole-4-carboxylate (Intermediate-**A**). Reaction of **1** with Intermediate-**A** under refluxing condition in ethanol afforded ethyl 1-(6-chloropyrimidin-4-yl)-5-methyl-1*H*-pyrazole-4-carboxylate (**2**) by a facile formation of pyrazole ring, which then underwent nucleophilic substitution using by benzylamine to afford ethyl 1-(6-(benzylamino)pyrimidin-4-yl)-5-methyl-1*H*-pyrazole-4-carboxylate (**3**). Hydrolysis of **3** using lithium hydroxide [25] yielded the corresponding acid (**4**) which then was coupled with respective amines using 1-hydroxybenzotriazole hydrate **(**HOBT) and 1-ethyl-3-(3-dimethylaminopropyl)carbodiimide hydrochloride (EDC HCl) reagent [26] to afford the target compounds in moderate to high yields involving facile workup procedures.

3.3. Biology

Synthesized target compounds were screened for their potential to inhibit CDK2/CyclinA2 enzymatic activity *in vitro*. Table 2 shows the results of the biochemical evaluation and Glide score values. While many compounds were found to be inactive (IC_{50}>100 μM), few compounds were found to be significantly potent as compared to the activity of roscovitine (IC_{50} = 0.32 μM). Of these, compounds **5b**, **5i**, **5j**, **5l** and **5m** were found to be significantly active with IC_{50}< 20 nM. In general, good agreement was found between Glide score and IC_{50} values. For example, compounds **5b**, **5i**, and **5j** which were found to have IC50 <15 nM had the highest scores amongst the predicted compounds. A closer analysis of structure-activity relationship suggests that both aromatic and aliphatic substituents were tolerated at the R_1 position. In general, irrespective of the positions at the aromatic ring (ortho/meta/para), polar groups and groups with H-bond donors (e.g. OH and NH) were found to decrease the activity. From the poses, it was expected that the activity would be mostly governed by dispersion interactions. Indeed, as seen from the activity of **5d**, **5i**, **5j**, **5m**, **5o**, **5p**, this was found to be the case.

Structure–activity relationship (SAR)

The substitution pattern of the aryl amine ring at the different position was observed to affect biological activity. The electronic nature of the substituents led to significant variation for disparity in activity. Compounds possessing electron-donating substituents Except -F (-OH, -OCH3) at 4th position of phenyl ring led to an increase in the CDK2-Cyclin A inhibition activity. The methyl group (weak electron donating) at 2nd, 3rd and 4th position of phenyl ring was found to be a less active. In particular, it was found that **5k** occupied a different position of R group than its close analogues: **5i**, **5j** and **5l**. As seen from Fig. 3a, 4-methylphenyl analog (**5k**) faces towards solvent while in **5i**, **5j** and **5l**, corresponding aryl moieties align well and interact with protein residues by dispersion interactions. This could be one of the reasons of **5k** being less scored and less active *in vitro*. Similarly, we tried to also hypothesize the differential activities between structurally close homologs; **5o**, **5p**, **5q** and **5r**. It was evident to see that bulky substitution was not tolerated at C-3 position of the phenyl ring at R group. Indeed, as seen from Fig. 3b, compound **5o** with 3-F substitution fit well in the protein allowing the aryl ring to have dispersion (CH-π) interactions with neighbouring residues. Increasing the bulk from fluoro to chloro (**5p**), methoxy (**5q**), methyl (**5r**) and acetyl (**5u**) moved the phenyl ring slightly out of the hydrophobic pocket facing the solvent side on account of steric clashes. Indeed, this was reflected in the reduced/loss of activity of **5q**, **5r** and **5u**. While **5p** did retain activity, we think that this may have resulted because of reasons which couldn't be explained by simple protein-ligand interactions (for example, entropic considerations or protein conformational change).

The phenyl ring without any electron donating or withdrawing group also showed weaker CDK2-Cyclin A inhibitory activity. Furthermore, compounds having electron-donating substituents (-Me, -OMe, -OH) at 3rd position of phenyl ring to a decrease in the CDK2-Cyclin A inhibition activity, except halogenated groups (-Cl & -F). In addition, compound possessing -COCH3 group at 3rd position of phenyl ring led to a decrease in the CDK2-Cyclin A inhibition activity. In contrast, compounds bearing electron donating groups (–Cl, -OMe, -Me, -OH, -F) at 2nd position of phenyl ring possessed weaker activity. It can be noted that among the halogenated compounds with the lowest lipophilicity (Lowest Log P) showed highest activity.

Compounds having aliphatic amines also showed excellent CDK2-Cyclin A inhibitory activity. Compounds possessing piperidine, morpholine & ethanolamine led to more potent CDK2-Cyclin A inhibitory activity. While compounds containing piperidone and piperazine afforded weaker CDK2-Cyclin A inhibitory activity. Furthermore, CDK2-Cyclin A inhibitory activity was observed, when compound possess *N*-methylpiperazine. While ethyl substituted compounds showed lesser activity. Compounds possessing benzyl amine, isoniazid and phenyl hydrazine as substituents were also found to lesser CDK2-Cyclin A inhibitory activity. This concept has been explained graphically in fig. 4.

4. Conclusions

In conclusion, a series of novel pyrimidine-pyrazole hybrid molecules as potent CDK2-CyclinA2 enzyme inhibitors has been studied. Molecular docking of these novel molecules on CDK2-CyclinA2 enzyme (PDB: 2R3J) exhibited very good docking score values which was also confirmed by the biochemical assay using a luminescent ADP detection method. On the basis of SAR, it has been observed that compounds having electron donating fluoro and chloro groups on aryl amine as well

as piperidine and morpholine show increased CDK2-Cyclin A inhibitory activities. Out of total 26 compounds synthesized and screened, at least 5 compounds were found to be highly potent (IC_{50} < 20 nM); which are very good candidates for further optimization of drug likeliness and selectivity over other kinase isoforms.

Conflicts of interest

The authors declare that they have no competing interests.

Acknowledgement

This work was supported by the Gujarat Council on Science and Technology (**GUJCOST/MRP/14-15/1138**), Department of Science and Technology, Gandhinagar, Gujarat, India. Mayur K. Vekariya is also thankful to the UGC, India for providing financial support under UGC-BSR Fellowship (Grant No: F./25-1/2013- 14 (BSR) / 7-74/2007 (BSR) dated 30-05- 2014).

List of Figure legends

Fig. 1: Examples of CDK2 inhibitors in clinical evaluation

Fig. 2: Interactions of the target compounds **5i** (panel a) and **5j** (panel b) with CDK2 protein (PDB Code 2R3J). Color coding: carbon in cyan (protein) or yellow (ligand), nitrogen in blue, oxygen in red. The numbers represent distances in Å.

Fig. 3: Panel a) Poses of target compounds **5i**, **5j**, **5k** and **5l** in CDK2. Color coding: carbon in cyan (**5j**), green (**5l**), orange (**5i**) and yellow (**5k**); nitrogen in blue, oxygen in red, fluorine in off-white; Panel b) Poses of target compounds **5o**, **5p**, **5q** and **5r** in CDK2. Color coding: carbon in green (**5o**), orange (**5p**), yellow (**5q**) and pink (**5r**), nitrogen in blue, oxygen in red, fluorine in off-white.

Fig. 4: Structure–activity relationship

References

[1] T. M. Sielecki, J. F. Boylan, P. A. Benfield, G. L. Trainor, *J. Med. Chem.* **2000**, *43*, 1.

[2] S. Lapenna, A. Giordano, *Nat. Rev. Drug Discov.* **2009**, *8*, 547.

[3] T. O. Fischmann, A. Hruza, J. S. Duca, L. Ramanathan, T. Mayhood, W. T. Windsor, et al., *Biopolymers* **2008**, *89*, 372.

[4] G. Mariaule, P. Belmont, *Molecules* **2014**, *19*, 14366.

[5] E. B. Skibo, X. Huang, R. Martinez, R. H. Lemus, W. A. Craigo, R. T. Dorr, *J. Med. Chem.* **2002**, *45*, 5543.

[6] A. Balbi, M. Anzaldi, C. Macciò, C. Aiello, M. Mazzei, R. Gangemi, et al., *Eur. J. Med. Chem.* **2011**, *46*, 5293.

[7] V. Sullivan, C. L. Talarico, S. C. Stanat, M. Davis, D. M. Coen, K. K. Biron, *Nature* **1992**, *358*, 162.

[8] O. I. El-Sabbagh, M. M. Baraka, S. M. Ibrahim, C. Pannecouque, G. Andrei, R. Snoeck, et al., *Eur. J. Med. Chem.* **2009**, *44*, 3746.

[9] H. Mitsuya, K. J. Weinhold, P. A. Furman, M. H. S. Clair, S. N. Lehrman, R. C. Gallo, et al., *Proc. Natl. Acad. Sci.* **1985**, *82*, 7096.

[10] C. E. Mowbray, C. Burt, R. Corbau, S. Gayton, M. Hawes, M. Perros, et al., *Bioorg. Med. Chem. Lett.* **2009**, *19*, 5857.

[11] M. C. Koshy, D. Mickley, J. Bourgiognie, M. D. Blaufox, *Circulation* **1977**, *55*, 533.

[12] V. P. Arya, R. S. Grewal, C. L. Kaul, S. P. Ghate, D. V. Mehta, T. George, *J. Pharm. Sci.* **1969**, *58*, 432.

[13] Y. L. Janin, *Bioorg. Med. Chem.* **2007**, *15*, 2479.

[14] H. K. Maurya, R. Verma, S. Alam, S. Pandey, V. Pathak, S. Sharma, et al., *Bioorg. Med. Chem. Lett.* **2013**, *23*, 5844.

[15] J. Majeed, M. Shaharyar, *J. Enzyme Inhib. Med. Chem.* **2011**, *26*, 819.

[16] A. Chauhan, P. K. Sharma, N. Kaushik, *Int J ChemTech Res* **2011**, *3*, 11.

[17] A. Foroumadi, S. Emami, A. Hassanzadeh, M. Rajaee, K. Sokhanvar, M. H. Moshafi, et al., *Bioorg. Med. Chem. Lett.* **2005**, *15*, 4488.

[18] A. A. Bekhit, T. Abdel-Aziem, *Bioorg. Med. Chem.* **2004**, *12*, 1935.

[19] A. Polak, H. J. Scholer, *Chemotherapy* **1975**, *21*, 113.

[20] V. K. Tandon, D. B. Yadav, A. K. Chaturvedi, P. K. Shukla, *Bioorg. Med. Chem. Lett.* **2005**, *15*, 3288.

[21] S. Furukawa, K. Usuda, Y. Fujieda, T. Tamura, Y. Miyamoto, K. Hayashi, et al., *J. Vet. Med. Sci.* **2000**, *62*, 23.

[22] D. Sowjanya, D. Sowndarya, N. Mounika, K. N. Jyothi, P. S. N. Lakshmi, B. S. Sree, et al., .

[23] M. Koresawa, T. Okabe, *ASSAY Drug Dev. Technol.* **2004**, *2*, 153.

[24] S. Al-Mousawi, E. John, M. M. Abdelkhalik, M. H. Elnagdi, *J. Heterocycl. Chem.* **2003**, *40*, 689.

[25] B. Dayal, G. Salen, B. Toome, G. S. Tint, S. Shefer, J. Padia, *Steroids* **1990**, *55*, 233.

[26] L. A. Carpino, A. El-Faham, F. Albericio, *J. Org. Chem.* **1995**, *60*, 3561.

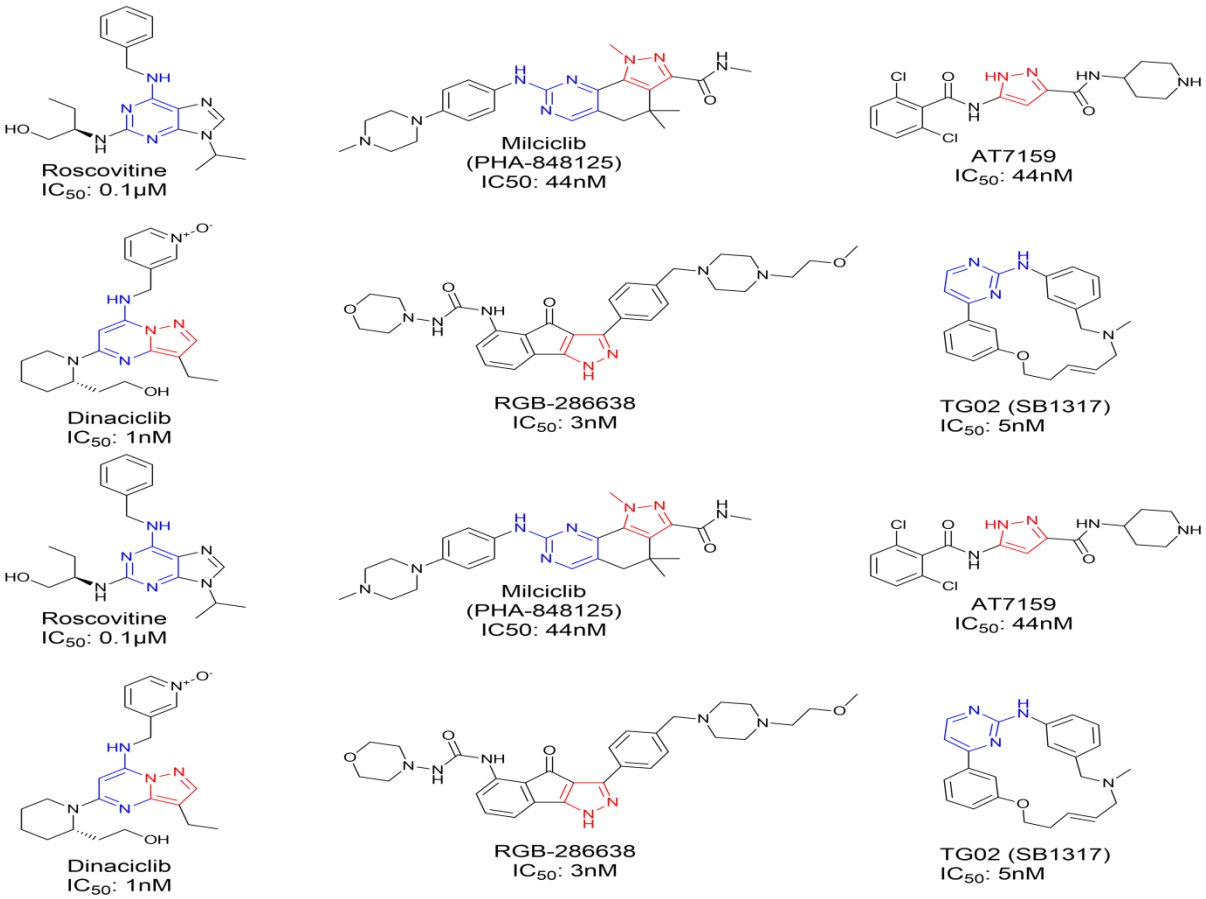

Fig. 1 Examples of CDK2 inhibitors in clinical evaluation

a) b)

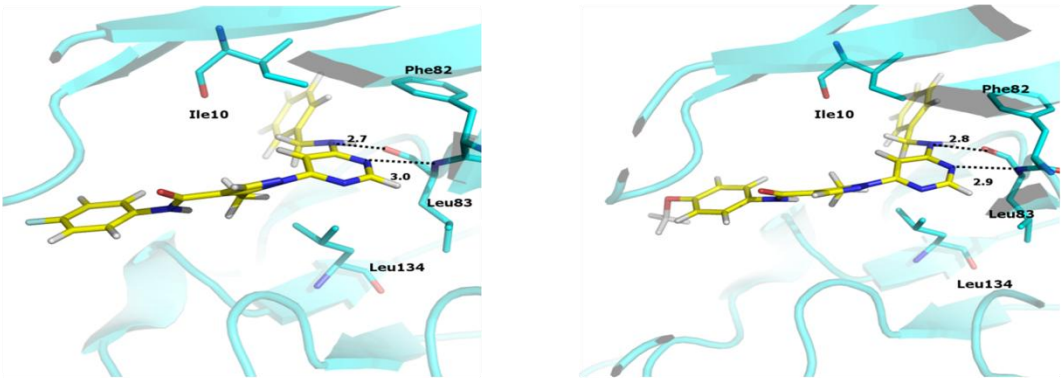

Fig. 2 Interactions of the target compounds **5i** (panel a) and **5j** (panel b) with CDK2 protein (PDB Code 2R3J). Color coding: carbon in cyan (protein) or yellow (ligand), nitrogen in blue, oxygen in red. The numbers represent distances in Å.

a) b)

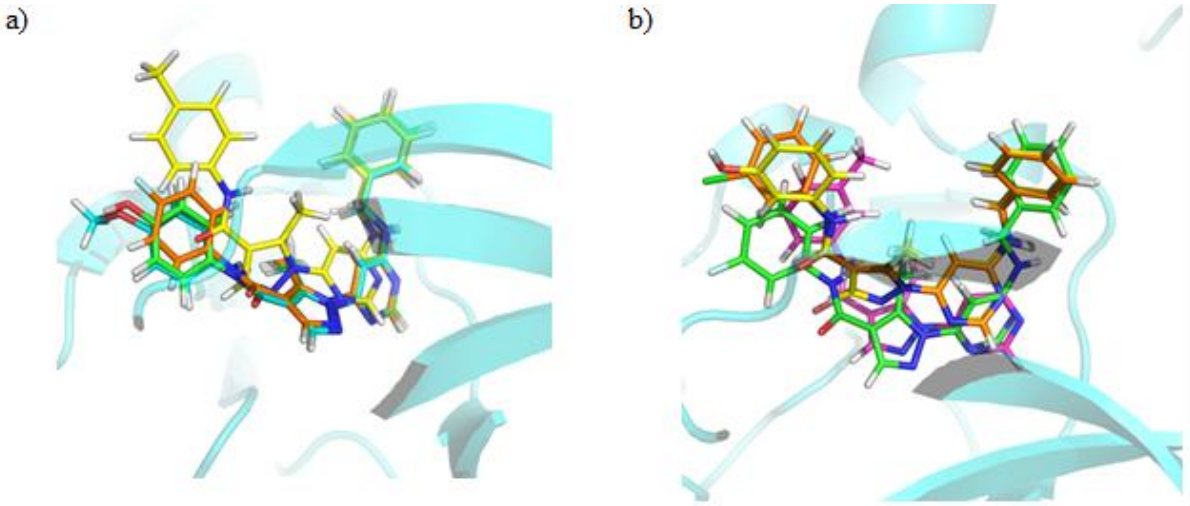

Fig. 3: Panel a) Poses of target compounds **5i**, **5j**, **5k** and **5l** in CDK2. Color coding: carbon in cyan (**5j**), green (**5l**), orange (**5i**) and yellow (**5k**); nitrogen in blue, oxygen in red, fluorine in off-white; Panel b) Poses of target compounds **5o**, **5p**, **5q** and **5r** in CDK2. Color coding: carbon in green (**5o**), orange (**5p**), yellow (**5q**) and pink (**5r**), nitrogen in blue, oxygen in red, fluorine in off-white.

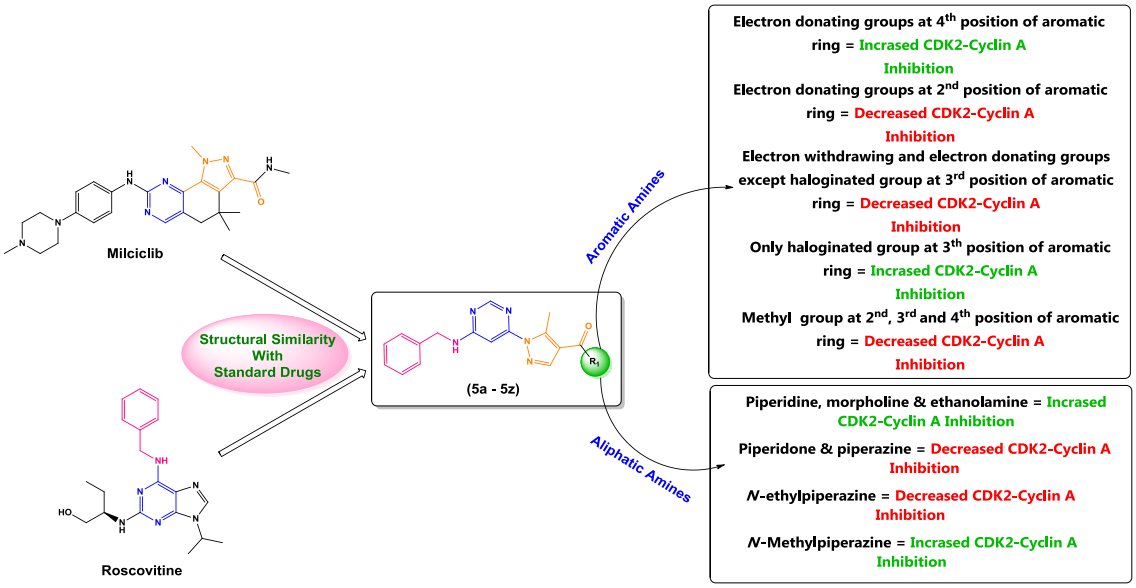

Fig. 4 Structure–activity relationship

Synthesis of Intermediate-A

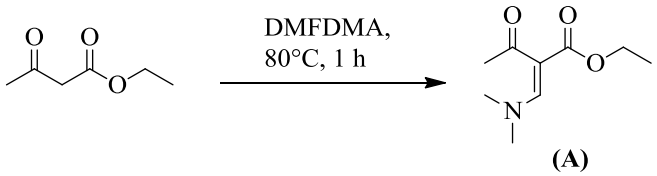

(A)

Synthesis of target compounds

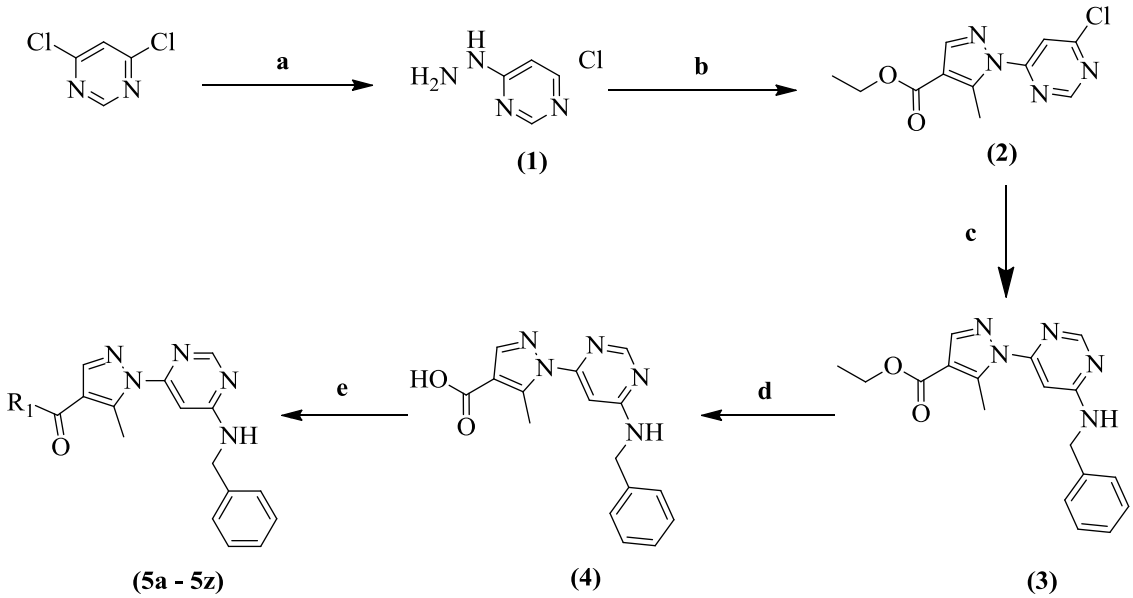

Scheme 1. Reagents and conditions: (a) $NH_2NH_2.H_2O$, EtOH, 1.5 h, rt; (b) Intermediate-A, EtOH, 1 h, reflux; (c) Benzylamine, TEA, EtOH, 3 h, reflux; (d) LiOH, MeOH, H_2O, 24 h, reflux; (e) various amines, HOBt, EDC.HCl, DIPEA, DMF, 1-2 h, reflux.

Table 1 : Pharmacokinetic properties of compounds 5a-5z

	Lipinski's rule of five factors						Pharmacokinetic properties			
Comp	Mol_MW (<500)	Donor HB (<5)	Acceptor HB (<10)	QP log Po/w (<5)	Molar Refractivity	Rule of five	Percent human oral absorption (>80 high, <25 poor)	QP log S[a] (-6.5 to 0.5)	QP logHERG[b] (below -5)	QPlog BB[c] (-3 to 1.2)
5a	384	2	6	4.559	112.2	0	100	-6.575	-7.852	-0.788
5b	378	1	7	3.199	104.54	0	100	-4.867	-6.068	-0.48
5c	398	2	6	4.932	115.43	0	100	-6.913	-7.899	-0.811
5d	376	1	6	4.202	107.57	0	100	-6.261	-6.556	-0.609
5e	378	3	6	2.618	105.38	0	83.302	-4.643	-7.214	-0.516
5f	390	1	7	3.068	107.96	0	92.556	-5.622	-6.619	-1.21
5g	428	3	9	3.465	116.99	0	88.9	-6.181	-7.66	-1.805
5h	352	3	7	2.526	97.24	0	89.715	-4.625	-6.444	-1.336
5i	402	2	6	4.788	112.17	0	100	-6.914	-7.705	-0.673
5j	414	2	7	4.653	118.76	0	100	-6.795	-7.714	-0.871
5k	398	2	6	4.861	116.95	0	100	-7.133	-7.732	-0.814
5l	400	3	7	3.793	113.88	0	95.584	-6.251	-7.703	-1.477
5m	392	2	6	2.994	110.34	0	90.569	-4.276	-7.04	-0.186
5n	406	2	6	3.429	114.96	0	92.625	-5.012	-7.506	-0.34
5o	402	2	6	4.791	112.17	0	100	-6.932	-7.716	-0.682

5p	418	2	6	5.045	122.06	0	100	-7.294	-7.732	-0.631
5q	414	2	7	4.606	118.76	0	100	-6.545	-7.467	-0.768
5r	398	2	6	4.862	116.95	0	100	-7.127	-7.727	-0.812
5s	400	3	7	3.75	113.88	0	96.44	-6.017	-7.454	-1.363
5t	427	3	8	4.407	119.19	0	100	-6.851	-7.862	-1.49
5u	426	2	7	3.999	122.22	0	100	-6.581	-7.533	-1.399
5v	402	2	6	4.812	112.17	0	100	-6.966	-7.789	-0.688
5w	414	2	7	4.71	118.76	0	100	-6.891	-7.765	-0.883
5x	418	2	6	5.026	122.01	1	100	-7.175	-7.728	-0.6
5y	398	2	6	4.825	116.95	0	100	-6.935	-7.638	-0.773
5z	400	3	7	3.826	113.88	0	100	-5.981	-7.447	-1.256

[a] Predicted aqueous solubility in mol/l , [b] Predicted IC_{50} value of HERG K^+ channels blockage, [c] Predicted blood–brain barrier permeability

Table 2: Inhibition of CDK2-Cyclin A activity by the target compounds

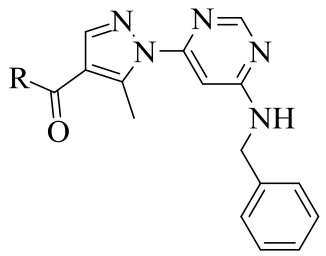

(5a - 5z)

Compound	R	Glide-XP Score	CDK2/CyclinA2 IC_{50} (µM)	Compound	R	Glide-XP Score	CDK2/CyclinA2 IC_{50} (µM)
5a	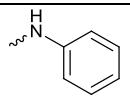	-6.896	>100	5n	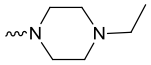	-6.599	>100
5b	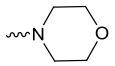	-8.966	0.008 ± 0.014	5o	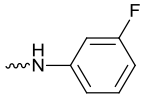	-7.649	0.067 ± 0.014
5c	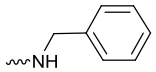	-6.765	>100	5p	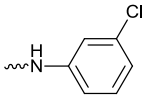	-6.449	0.074 ± 0.001
5d	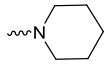	-8.759	0.022 ± 0.022	5q	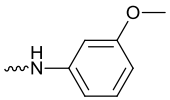	-6.235	>100
5e	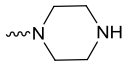	-6.586	>100	5r	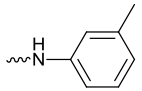	-6.556	>100

5f	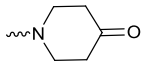	-6.445	>100	5s	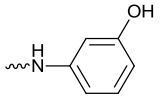	-8.645	>100
5g	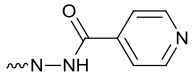	-6.836	>100	5t	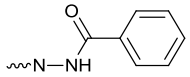	-6.300	>100
5h	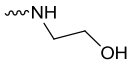	-7.234	0.1 ± 0.002	5u	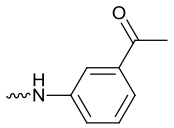	-6.412	>100
5i	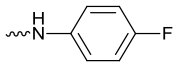	-8.783	0.015 ± 0.015	5v	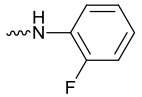	-7.828	>100
5j	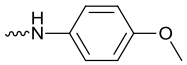	-9.014	0.015 ± 0.010	5w	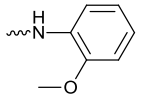	-7.850	>100
5k	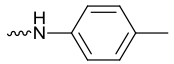	-6.932	>100	5x	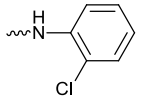	-7.818	>100
5l	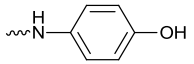	-7.704	0.01 ± 0.002	5y	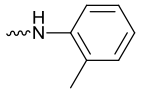	-7.986	>100
5m	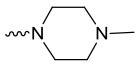	-7.739	0.018 ± 0.012	5z	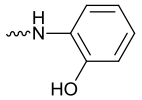	-7.123	>100
Roscovitine	---	-8.866	0.34 ± 0.035				